

## Roughness of Interfacial Crack Fronts: Stress-Weighted Percolation in the Damage Zone

Jean Schmittbuhl\* and Alex Hansen†

*International Center for Condensed Matter Physics, Universidade de Brasília, 70919-970 Brasília, Distrito Federal, Brazil*

G. George Batrouni‡

*Institut Non-Linéaire de Nice, UMR CNRS 6618, Université de Nice-Sophia Antipolis,  
1361 Route des Lucioles, F-06560 Valbonne, France*

(Received 22 July 2002; published 31 January 2003)

We study numerically the roughness exponent  $\zeta$  of an in-plane fracture front slowly propagating along a heterogeneous interface embedded in an elastic body, using a model based on the evolution of a process zone rather than a fracture line. We find  $\zeta = 0.60 \pm 0.05$ . For the first time, simulation results are in close agreement with experimental results. We then show that the roughness exponent is related to the correlation length exponent  $\nu$  of a stress-weighted percolation problem through  $\zeta = \nu/(1 + \nu)$ . A numerical study of the stress-weighted percolation problem yields  $\nu = 1.54$  giving  $\zeta = 0.61$  in close agreement with our numerical results and with experimental observations.

DOI: 10.1103/PhysRevLett.90.045505

PACS numbers: 62.20.Mk, 81.40.Np, 83.80.Ab

An important motivation for studying interfacial crack pinning [1,2] is to simplify the study of the origin of the scaling properties of brittle crack surfaces [3,4]. These scaling properties are seen, for example, in the width of the fracture  $w$  in the direction transverse to the average fracture plane, which behaves as

$$w \sim L^{\zeta_{\perp}}, \quad (1)$$

where  $L$  is the linear size of the fracture and  $\zeta_{\perp}$  is the roughness exponent. It is now generally believed that the roughness exponent shows a universal value of about 0.80 at longer length scales [5], while a lower value of about 0.5 might be seen at smaller scales [6].

Direct observations of the interfacial crack pinning have been performed recently. The problem consists of following the roughness of a crack front moving along the flat interface between two elastically connected blocks. The experimental study of constrained crack propagation between two sintered Plexiglas plates presented in [2] resulted in the estimate of the in-plane roughness exponent:  $\zeta = 0.55 \pm 0.05$ . This work was followed by a longer study leading to the estimate  $\zeta = 0.63 \pm 0.03$  [7]. A recent study of the motion of a helium-4 meniscus along a disordered substrate—a problem closely related to the motion of a crack line—gave  $\zeta = 0.56 \pm 0.03$  [8].

Numerous models for interfacial crack propagation in heterogeneous material have been proposed. The numerical simulation presented in [1] is based on a perturbative Green function approach following the quasistatic evolution of the interfacial crack front position  $a(x, t)$  [9], which is treated as a function of time,  $t$ , and as a single-valued function of position  $x$  along the orthogonal direction to the crack advancement direction. The linearized Green function used binds together points only along the fracture front. The stress intensity factor at a point  $x$  along the fracture front is then found to be

$$\frac{K(x, t)}{K_0} = 1 + \frac{1}{2\pi} \text{p.v.} \int_{-\infty}^{+\infty} \frac{a(x', t) - a(x, t)}{(x - x')^2} dx', \quad (2)$$

where  $K_0$  is the stress intensity factor that would result if the crack were straight [9]. The fracture is advanced by identifying the most stressed point along the fracture line and advancing this by a small step. The roughness exponent of the crack front was estimated numerically to be  $\zeta = 0.35$ , while a direct dynamical renormalization group calculation gave  $\zeta = 1/3$  to lowest order [10]. Higher-order corrections to this quasistatic analysis increases the value of  $\zeta$  to 0.48 [11], while a different quasistatic numerical technique suggests  $0.390 \pm 0.002$  [12]. Dynamic effects have been largely studied numerically and analytically [13], in particular, in the form of crack front waves. They lead to an increased roughness exponent compared to the initial  $1/3$  value up to  $\zeta = 0.5$  but still smaller than experimental observations. A numerical study using two-dimensional beam lattices also gave a roughness exponent close to  $1/3$  [14].

Hence, the situation today is that there is a large and significant discrepancy between theoretical and experimental estimates, theoretical estimates being considerably smaller than the experimental ones.

In this Letter we first present a numerical calculation of the roughness exponent of a crack front that propagates quasistatically along a heterogeneous interface, based on a Green function technique which differs from that previously used. Indeed, our model does not reduce the crack tip to a single tortuous line but describes the tip as a region of interactions between microcracks (see Fig. 1). Our technique is based on the static solution of the elastic equations for the deformation of the surface of an elastic half space [15]. The local deformation,  $u$ , at position  $(x, y)$  along the plane is related to the normal stress field  $\sigma$  by

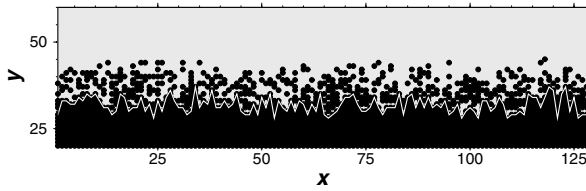


FIG. 1. The crack front for a  $128 \times 128$  system. The fracture is propagating from bottom to top. The broken springs are black dots. The crack front is drawn as a white line.

$$u(x, y) = \iint G(x - x', y - y') \sigma(x', y') dx' dy', \quad (3)$$

where the Green function is [16]

$$G(x, y) = \frac{1 - s^2}{\pi e} \frac{1}{|(x, y)|}, \quad (4)$$

with  $s$  the Poisson ratio and  $e$  the elastic constant.

For the sake of simplicity, as generally is done for the study of contact between two elastic bodies [16], we substitute one of the elastic plates by an infinitely rigid one. The other plate is modeled as an elastic block for which Eqs. (3) and (4) are valid. We discretize the model so that the forces and deformations are described by

$$u_i = \sum_j \bar{G}_{i,j} f_j, \quad (5)$$

where  $u_i$  is the deformation of the elastic body at site  $i$ , and  $f_i$  is the force acting at that point.  $\bar{G}_{i,j}$  is the Green function (4) averaged over an area  $b^2$ . The indices  $i$  and  $j$  run over all  $L^2 = L_x \times L_y$  sites.

The elastic block is connected to the infinitely stiff plate by a discrete interface made of an array of elastic harmonic springs. The springs are brittle and have breaking thresholds randomly drawn from a uniform distribution between zero and one. The spacing between the springs is  $b$  in both the  $x$  and  $y$  directions. The force  $f_i$  that an unbroken spring  $i$  is carrying is transferred over an area of size  $b^2$  to the soft surface and given by Hooke's law:

$$f_i = -k(u_i - D), \quad (6)$$

where  $k$  is the spring constant ( $k = 1$  for all springs).  $D$  is the displacement of the infinitely stiff medium and is a function of  $y$ , i.e., solid rotation of the stiff medium. The quantity  $(u_i - D)$  is, therefore, the length that spring  $i$  is stretched. We assume periodic boundary conditions both in the  $x$  and  $y$  directions.

In order to model the mode I fracturing of the interface between the two media [cantilever beam (CB) test] in a way compatible with the biperiodic boundary conditions, we let  $D(y) = \max[g_u(|y - L_y/2| - y_0), 0]$ , where  $g_u$  is the displacement gradient and is set to 0.01. The load  $y_0$  is decreased successively and as a result, the springs break

one by one (event driven algorithm). The numerical technique to solve the equations that ensue is presented in detail in [17].

When either  $L_x$  or  $L_y$  is changed, the elastic constant  $e$  is changed in such a way that  $\sum_{i,j} \bar{G}_{i,j}/L^2$  is kept fixed. The threshold distribution is also scaled by the same factor. This ensures that the local elastic properties of the system, both concerning the soft material and the fibers, remain unchanged.

We show in Fig. 1 a typical damage front in a  $128 \times 128$  system. We define the fracture front  $a(x, t)$  in this model as the set of nodes that form a continuous path separating the infinite cluster of broken springs from the infinite cluster of unbroken springs. This definition is similar to that of Ref. [2]. From Fig. 1, we clearly see that even when a front can be defined, an extended damage zone exists. Accordingly the front does not capture all the active tip of the fracture. This observation supports the relevance of a description of the crack front which is not based on the line model.

In Fig. 2, we show the width of the fracture front  $w = \sqrt{\langle a^2 \rangle - \langle a \rangle^2}$  as a function of its average position  $\langle a \rangle$ —which acts as a time parameter in this quasistatic model, for various system widths  $L_x$ , while keeping the system length  $L_y$  fixed. By collapsing the width evolution for the different system sizes, we see that the crack front follows a Family-Vicsek scaling [18]. Two important exponents are, thus, obtained: the roughness exponent  $\zeta = 0.60 \pm 0.05$  and the dynamical exponent  $z = 1.5 \pm 0.1$ . The roughness exponent is in excellent agreement with the experimentally obtained value [2,7,19,8], while the dynamical exponent  $z$  was found in Ref. [19] to be slightly lower:  $1.2 \pm 0.1$ .

Our model distinguishes itself from earlier numerical models in three major ways: (i) Most previous models are based on a small perturbation approach leading to the kernel in Eq. (2) which is linearized with respect to the

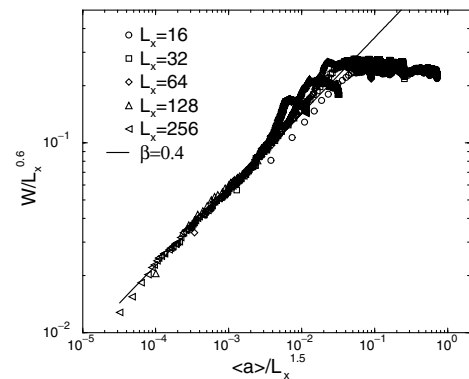


FIG. 2. Family-Vicsek scaling of the crack front roughness:  $w/L_x^\zeta$  vs  $\langle a \rangle/L_x^z$  for fixed length of the system,  $L_y = 128$ . We find  $\zeta = 0.6$  and  $z = 1.5$ . The slope of the straight line is  $\beta = 0.4$ , which is consistent with  $\beta = \zeta/z$  as expected in Family-Vicsek scaling.

shape of the crack front [9]. Such linearizations are not necessary in the present approach. (ii) It was assumed in the earlier studies that the fracture line was a single-valued function, hence ruling out overhangs. This assumption prevents islands of unbroken bonds from forming in the wake of the advancing fracture line. (iii) The assumption of a single advancing fracture line also prevents the formation of a damage zone in front of the fracture line. None of these three assumptions are necessary in the present model. In order to test whether assumptions (ii) or (iii) are responsible for the difference in the roughness exponent, we imposed both on the present model. No change in  $\zeta$  was observed. Hence, we conclude that it is the linearization assumption that is responsible for the difference.

The second part of this Letter is devoted to the establishment of a theoretical link between the roughness exponent  $\zeta$  and a stress-weighted percolation process in a gradient imposed by the mode I loading of the system. We start by characterizing the stress-weighted percolation. To this end, we consider a similar problem but where the loading is obtained without any gradient, i.e., horizontal and parallel displacement of the rigid medium [17]. In this case, when the homogeneous displacement  $D$  of the rigid medium reaches a maximum value,  $D_c$ , the system goes unstable, and unless  $D$  is decreased again, catastrophic failure sets in. In [17], the size distribution of clusters of broken springs was studied, and a power law was found with an exponent  $\tau = 1.6$ . This value is different from ordinary percolation where  $\tau \approx 2.05$  [20]. In Fig. 3, we show the fluctuations of density of broken springs at  $D = D_c$ . If there is a diverging correlation length in the problem, these fluctuations scale as  $L^{-1/\nu}$ . We find that  $1/\nu = 0.65$ , leading to  $\nu = 1.54$ . Hence, the fracture process in this system is in a universality

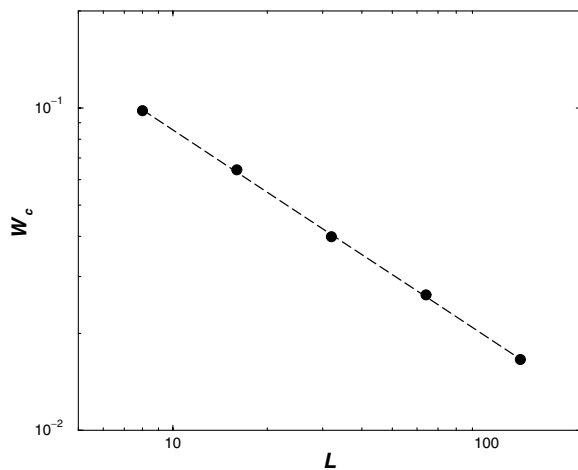


FIG. 3. Fluctuations of the density of broken bonds  $W_c = (\langle p_c^2 \rangle - \langle p_c \rangle^2)^{1/2}$  plotted against  $L$  for a homogeneous parallel loading without any gradient, i.e., constant  $D$  over the whole system. The slope of the straight line is  $-1/\nu = -0.65$ .

class which is *different* from standard percolation where  $\nu = 4/3$ .

When  $D$  is no longer spatially constant but is given by CB load, the form of interactions between the springs does not change. Hence, the critical properties of the model when run in the “horizontal” mode are still present under CB loading. The wedge shape of  $D$  leads to a gradient in the loading of the springs, going from very high loading where the damage is large to very low loading well into the still intact part of the interface. In Fig. 4, we show the damage profile  $p(y)$ , i.e., the density of broken springs averaged in the  $x$  direction, for systems of different sizes. The profile is clearly linear in a finite region. Somewhere along this damage profile, there is a line in the  $x$  direction at  $y = y_c$  where the damage density is critical,  $p(y_c) = p_c$ . In the vicinity of this line, there is a critical region which is characterized by being on the edge between stability and instability and corresponds to the crack front. Following the arguments of Sapoval *et al.* for percolation in a gradient [21], if  $p(y)$  follows a linear law around  $p_c$  (when ignoring small corrections for finite-size systems) as shown in Fig. 4,

$$p(y) = p_c - \frac{y - y_c}{l_y}, \tag{7}$$

where  $l_y$  is the width of the damage zone and defined as the scale over which  $p(y)$  goes from 1 to zero. The critical region has a width  $\xi = |y_w - y_c|$  which is related to the damage  $p(y_w)$  as  $\xi \sim |p(y_w) - p_c|^{-\nu}$ . Introducing  $\xi$  in Eq. (7) gives

$$\xi \sim l_y^{\nu/(1+\nu)}. \tag{8}$$

The influence of damage at some location is transmitted to the surroundings by a rotationally symmetric Green function (4). The externally imposed load on the

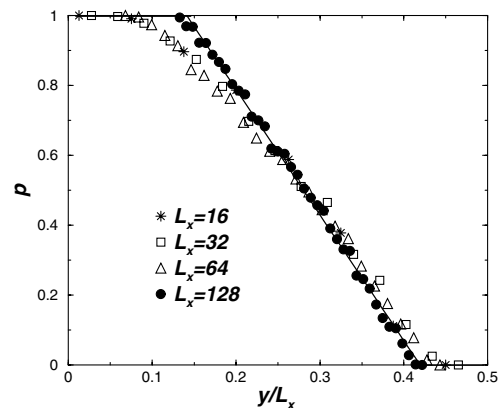


FIG. 4. Damage profile  $p(y/L_x)$  in reduced variable  $y/L_x$  for three different system widths  $L_x$  and fixed system length  $L_y = 128$ . Averaging over many samples and positions of the damage front has been performed by keeping the average position of the damage front fixed.

system introduces the gradient and corresponding length scale  $l_y$  in the damage.  $l_y$  is *independent* of the length of the system,  $L_y$ , while it depends linearly on the width of the system  $L_x$  by a mechanism similar to the one described in [22]. Hence,

$$l_y \propto L_x. \quad (9)$$

In Fig. 4, the reduced variable  $y/L_x$  was used resulting in data collapse for different system widths while keeping  $L_y$  fixed, thus validating Eq. (9). Furthermore, the width of the fracture front,  $w$ , is proportional to the width of the critical region  $\xi \propto w$ . Hence, we find

$$w \sim L_x^{\nu/(1+\nu)} = L_x^{0.61}, \quad (10)$$

where we have used our estimate  $\nu = 1.54$ . This result is in excellent agreement with our numerical simulations and with the experimental results.

A similar idea has been proposed for the outplane roughness of fracture surfaces where the gradient and the  $\nu$  exponent are different and leads to  $\zeta_{\perp} = 4/5$  in excellent agreement with the experimental value 0.80 [22]. We finally note that Zapperi *et al.* [23] have pointed out the connection between gradient percolation and the interface fracture problem in the limit of infinitely stiff plates. In that case, however, there is no equivalent of Eq. (9), and, consequently, there is no self-affinity. We have shown in this Letter that when the plates do respond elastically, the crack front is self-affine and that the universality class of the corresponding stress-weighted percolation problem is different from ordinary percolation.

This work was partially funded by the CNRS PICS Contracts No. 753 and No. 1373 and by the Norwegian Research Council, NFR. J. S. and A. H. thank Fernando A. Oliveira and the ICCMP for financial support during their stay in Brasília. J. S. was partly supported by the ACI “Jeunes Chercheurs” of the French Educational Ministry. Discussions with M. Alava, M. Bouchon, K. J. Måløy, S. Roux, and R. Toussaint are gratefully acknowledged.

---

\*Permanent address: Département de Géologie, UMR CNRS 8538, Ecole Normale Supérieure, 24, rue Lhomond, F-75231 Paris Cédex 05, France.

Electronic address: schmittb@geologie.ens.fr

†Permanent address: Department of Physics, NTNU, N-7491 Trondheim, Norway.

Electronic address: Alex.Hansen@phys.ntnu.no

‡Electronic address: george.batrouni@inln.cnrs.fr

- [1] J. Schmittbuhl, S. Roux, J. P. Vilotte, and K. J. Måløy, *Phys. Rev. Lett.* **74**, 1787 (1995).
- [2] J. Schmittbuhl and K. J. Måløy, *Phys. Rev. Lett.* **78**, 3888 (1997).
- [3] B. B. Mandelbrot, D. E. Passoja, and A. J. Paullay, *Nature (London)* **308**, 721 (1984).
- [4] S. R. Brown and C. H. Scholz, *J. Geophys. Res.* **90**, 12 575 (1985).
- [5] E. Bouchaud, G. Lapasset, and J. Planés, *Europhys. Lett.* **13**, 73 (1990); K. J. Måløy, A. Hansen, E. L. Hinrichsen, and S. Roux, *Phys. Rev. Lett.* **68**, 213 (1992); J. Schmittbuhl, S. Gentier, and S. Roux, *Geophys. Res. Lett.* **20**, 639 (1993); B. L. Cox and J. S. Y. Wang, *Fractals* **1**, 87 (1993); J. Schmittbuhl, F. Schmitt, and C. H. Scholz, *J. Geophys. Res.* **100**, 5953 (1995).
- [6] P. Daugier, S. Henaux, E. Bouchaud, and F. Creuzet, *Phys. Rev. E* **53**, 5637 (1996); P. Daugier, B. Nghiem, E. Bouchaud, and F. Creuzet, *Phys. Rev. Lett.* **78**, 1062 (1997).
- [7] A. Delaplace, J. Schmittbuhl, and K. J. Måløy, *Phys. Rev. E* **60**, 1337 (1999).
- [8] A. Prevost, E. Rolley, and C. Guthmann, *Phys. Rev. B* **65**, 064517 (2002).
- [9] H. Gao and J. R. Rice, *J. Appl. Mech.* **56**, 828 (1989).
- [10] D. Ertas and M. Kardar, *Phys. Rev. E* **49**, 2532 (1994).
- [11] P. Chauve, P. Le Doussal, and K. J. Wiese, *Phys. Rev. Lett.* **86**, 1785 (2001).
- [12] A. Rosso and W. Krauth, *Phys. Rev. E* **65**, 025101 (2002).
- [13] G. Perrin and J. R. Rice, *J. Mech. Phys. Solids* **42**, 1047 (1994); S. Ramanathan and D. S. Fisher, *Phys. Rev. Lett.* **79**, 877 (1997); *Phys. Rev. B* **58**, 6026 (1998); J. W. Morrissey and J. R. Rice, *J. Mech. Phys. Solids* **46**, 467 (1998); **48**, 1229 (2000).
- [14] J. Åström, M. Alava, and J. Timonen, *Phys. Rev. E* **62**, 2878 (2000).
- [15] L. Landau and E. M. Lifshitz, *Theory of Elasticity* (Clarendon Press, Oxford, 1958).
- [16] K. L. Johnson, *Contact Mechanics* (Cambridge University Press, Cambridge, 1985).
- [17] G. G. Batrouni, A. Hansen, and J. Schmittbuhl, *Phys. Rev. E* **65**, 036126 (2002).
- [18] F. Family and T. Vicsek, *J. Phys. A* **18**, L75 (1985).
- [19] K. J. Måløy and J. Schmittbuhl, *Phys. Rev. Lett.* **87**, 105502 (2001).
- [20] D. Stauffer and A. Aharony, *Introduction to Percolation Theory* (Taylor & Francis, London, Washington, D.C., 1992).
- [21] B. Sapoval, M. Rosso, and J. F. Gouyet, *J. Phys. (Paris), Lett.* **46**, L149 (1985).
- [22] A. Hansen and J. Schmittbuhl, cond-mat/0207360.
- [23] S. Zapperi, H. J. Herrmann, and S. Roux, *Eur. Phys. J. B* **17**, 131 (2000).